



Static strain aging and dislocation–impurity interactions in irradiated mild steel

K.L. Murty^{a,*}, I. Charit^b

^aNorth Carolina State University, Raleigh, NC 27695, USA

^bUniversity of Idaho, Moscow, ID 83844, USA

A B S T R A C T

Interactions between dislocations and interstitial impurity atoms lead to strain aging phenomenon in ferritic steels that are affected by the defects produced during neutron radiation exposure. We present here results on static strain aging in a silicon-killed mild steel before and after neutron irradiation. It is noted that the degree of strain aging (as measured by the yield point following restraining) decreased with increasing neutron dose resulting in essentially non-aging type at the highest dose ($\sim 10^{19}$ n/cm²). The strain aging kinetics were investigated using data at various aging temperatures and were found to be unaffected by the neutron radiation exposure. These experimental results are compared to those observed in dry hydrogen treated (partially denitrided) samples and are correlated with models on Cottrell locking.

© 2008 Elsevier B.V. All rights reserved.

1. Introduction

Strain aging is a type of mechanical behavior that is intimately associated with the well-known yield point phenomenon, observed especially in low carbon steels (ferritic steels). It refers to the increase in strength with concomitant reduction in ductility on heating to a relatively low temperature after cold working. This behavior is schematically illustrated in Fig. 1(a) [1]. Region A shows the stress–strain curve going through the usual yield point phenomenon to a plastically deformed state X. Then the specimen is unloaded and retested without any time delay or heat treatment. Upon reloading, no further yield point appears in the XY section (Region B) as the dislocations have already been torn away from the interstitial impurity atmospheres during the yield point phenomenon and Luder's strain. After the specimen is unloaded from Y and reloaded only after aging for several days at room temperature or several hours at around 148 °C, not only the yield point reappears but also the strength level is increased (Region C) and small Luder's band propagation is noted. The return of yield point is attributed to the diffusion of carbon and nitrogen (interstitial) atoms to the dislocations during the aging to lock them again by forming solute atmospheres [1,2]. The interstitial atoms are potent agents for causing strain aging effects because of their high diffusivity in body-centered cubic (bcc) crystal structure and their high interaction energies with dislocations [3]. This particular phenomenon is known as static strain aging (SSA) to differentiate it from another strain aging phenomenon known as dynamic strain aging (DSA). DSA is mainly observed during tensile straining due to the periodic locking and unlocking of dislocations by impurity atmo-

spheres. This has been adequately discussed in prior publications [4,5].

In Fig. 1(a) the increase in the stress during reloading ($\Delta\sigma$) is taken as the strain aging index and stronger the locking of the dislocations, higher the stress increment. This stress increment can be related to the concentration of interstitial impurity atoms that migrated to the dislocations. Another way to determine SSA characteristics is through unloading during Luder's strain and reloading, and evaluating the stress increment during initial Luder's band propagation as noted in Fig. 1(b). Following Hall and coworkers [6,7], the aging parameter (f) is defined by

$$f = \frac{\sigma'' - \sigma_0}{\sigma_0} = \frac{\Delta\sigma}{\sigma_0}, \quad (1)$$

where σ_0 is the lower yield stress at room temperature and σ'' the upper yield stress after aging and restraining at room temperature during Luder's band propagation. This method thus involves propagation of Luder's band, strain aging under zero load and room temperature unlocking of Luder's band. The main advantage of this method is that a limited number of samples are enough to obtain an adequate amount of data on the temperature and aging time dependences of the strain aging index f , thus minimizing specimen-to-specimen scatter.

When materials are exposed to intense neutron radiation, a large number of radiation-produced defects (vacancies, self-interstitials, dislocations and dislocation loops) are generated. Hall and others [2,8–10] have clearly demonstrated that the interstitial impurities combine with the radiation-produced defects (vacancies and interstitials) to form complexes, which may contribute partly to the total strengthening. At the same time, it has been noted that the net concentration of interstitial impurity atoms in solution decreases as a result of these interaction effects, and thus

* Corresponding author. Tel.: +1 919 515 3657; fax: +1 919 515 5115.
E-mail address: murty@ncsu.edu (K.L. Murty).

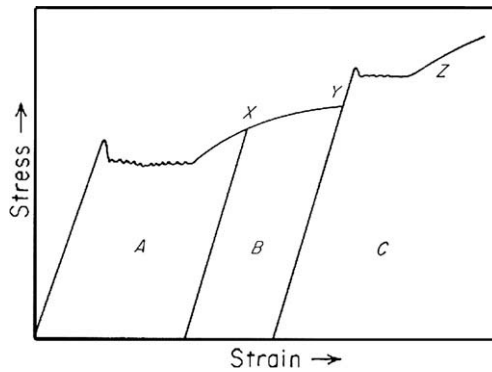


Fig. 1a. Schematic stress–strain curves illustrating strain aging effects [1].

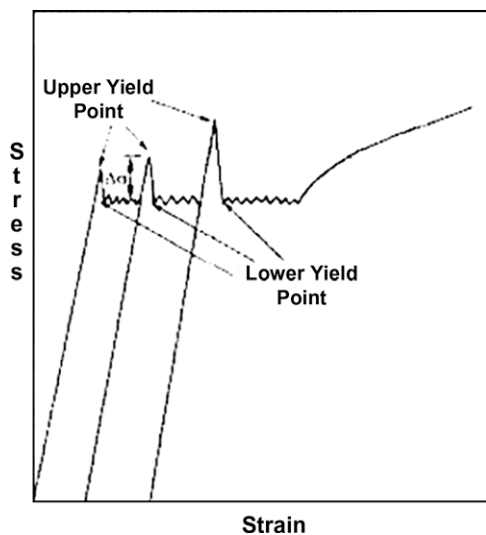


Fig. 1b. Alternate method [6,7] for evaluating SSA kinetics.

may make a steel fully non-aging if irradiated to sufficiently high neutron doses [9]. These affect the mechanical properties such as radiation hardening and embrittlement. Now the question arises as to how these interactions may be influenced while strain aging is simultaneously operating. The synergistic effects between DSA and radiation-produced defects have already been discussed elsewhere [4,5]. In this paper, we report how the SSA behavior responds to neutron radiation exposure. In slowly cooled and annealed mild steel, the majority of carbon precipitates as cementite while nitrogen becomes the dominant interstitial species responsible for strain aging [6]. Thus we studied the effect of partial denitriding on SSA kinetics and compare them to that of radiation exposure.

2. Experimental

Mild steel wires of 1 mm diameter and 38.5 mm gauge length were used as specimens in this study. The composition of the silicon-killed mild steel was Fe–0.05C–0.004N–0.012O–0.002Al–0.032Ni–0.39Ni–0.39Mn–0.012S–0.041Cr–0.09Cu–0.003Sn–<0.001Si (wt%). The specimens were annealed in vacuum at different temperatures for different times in order to obtain various grain sizes in the range from 27 to 53 μm .

The vacuum annealed samples were irradiated in the high-isotope flux Australian reactor (HIFAR) at Lucas height. Various

Table 1
Nitrogen concentration vs. annealing time

Series	Time, s (min) (at 675 °C)	Nitrogen (at%)
0	0	0.0160
1	4500 (75)	0.0960
2	8400 (140)	0.0044
3	10,800 (180)	0.0020
4	18,000 (300)	0.0014

neutron doses were obtained by placing the specimens at different locations from the fuel plates with different neutron fluxes. Corresponding neutron fluxes were calculated from the γ -activity of ^{46}Ti wire monitors placed along with the specimens. However, the irradiation time was kept constant in all the cases. Thus, a number of fluences were obtained: 3.9×10^{16} , 2.8×10^{17} , 2.0×10^{18} and 1.4×10^{19} n/cm² (energy > 1 MeV). Irradiation temperature was approximately 80 °C. All the irradiated specimens were stored in lead coffins until the γ -activity became minimal and considered safe for handling before tensile testing.

Partial denitriding of samples was achieved by annealing some specimens at 675 °C in a furnace with a dry hydrogen gas atmosphere followed by vacuum annealing at 500 °C for homogenization and to maintain a constant grain size. In all cases, specimens were furnace cooled so that no other aging effects (such as quench aging) can influence the mechanical behavior. Different levels of nitrogen were thus obtained. Table 1 summarizes the nitrogen concentration levels in the steel after the denitriding operation determined by chemical means and thus they represent the total nitrogen concentration comprising that in solution and the nitride precipitates.

All tensile tests were performed on a 'hard' tensile machine as proposed and designed by Adams [11] with relatively high machine modulus so that yield points during plastic deformation can be distinctly observed. The majority of the tensile tests were carried out at a cross-head speed of 5.2×10^{-3} mm s⁻¹, which was equivalent to nominal strain rate of 1.35×10^{-4} s⁻¹. The desired temperature during testing was maintained within ± 1 °C keeping the test specimen and assembly in an electrically heated oil or salt bath. SSA was carried out using the method illustrated by Eq. (1) on mild steel wires following vacuum annealing, dry hydrogen treatment (partial denitriding) and neutron radiation exposure to varied fluences.

3. Results and discussion

3.1. Radiation hardening

Before we discuss the SSA effects, it is important to briefly discuss the radiation hardening. Stress–strain curves are shown in Fig. 2 for the irradiated mild samples (average grain size of 27 μm) tested at 22 °C. The stress–strain curve for an unirradiated specimen is also shown to illustrate the effect of neutron radiation exposure. The strength of the material increased as a function of neutron fluence accompanied with reduced elongation to fracture. We note that Luder's strain increased with radiation fluence while rounded yield is noted at the highest fluence (1.4×10^{19} n/cm²). It turns out that at this fluence level, the sample failed during Luder's propagation itself.

Radiation hardening as noted by the increase in the lower yield stress, is observed to follow a power law dependence on neutron fluence, with the best fit obtained for a power of one-third (Fig. 3). It should be mentioned here that the experimental data fit one-third law better than square root dependence [4,5,12]. Luder's strain also followed the same dependence, as expected, since Luder's elongation in mild steel is known to be proportional

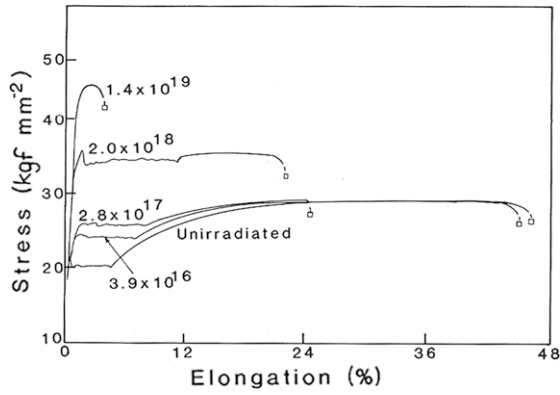


Fig. 2. Stress–strain curves for the mild steel specimens (average grain size 27 μm) at ambient.

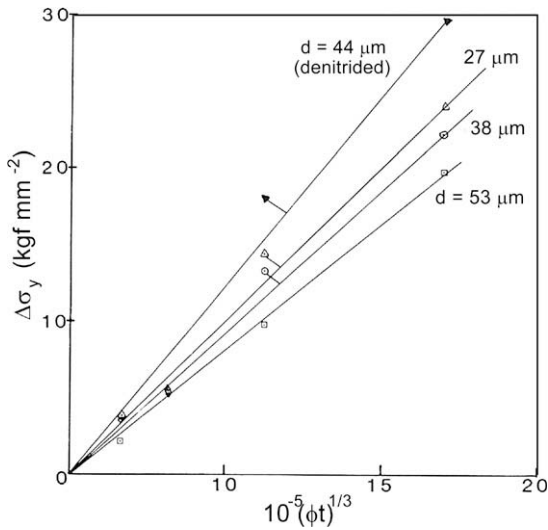


Fig. 3. Strength increment as a function of neutron fluence for mild steel for different grain sizes.

to the yield strength. It is interesting to note that both vacuum annealed and denitrated samples follow the same fluence dependence:

$$\sigma_{LY}^i - \sigma_{LY}^u = A(\phi t)^{1/3}, \tag{2}$$

where σ_{LY}^i and σ_{LY}^u are the lower yield stresses under irradiated and unirradiated conditions, ϕt is the neutron fluence (where ϕ is the neutron flux and t the radiation exposure time) and A is a constant. Table 2 summarizes the constant A for each grain size. The A values decrease with increasing grain size, implying that the extent of the radiation hardening becomes less in materials with coarser grain size. In other words, the coarser grained materials are more resistant to radiation damage; alternately finer grain sized materials are relatively more sensitive to radiation exposure. Since the initial dislocation density is inversely dependent on the grain size, it is

Table 2
Values of the constant 'A' (Eq. (2)) as a function of grain size in mild steel

Grain size (μm)	A (kg f/mm ²) (neutrons cm ⁻²) ^{-1/3}
27	10.15 × 10 ⁻⁶
38	9.35 × 10 ⁻⁶
53	8.30 × 10 ⁻⁶

possible that the starting dislocation density might have an effect on radiation sensitivity. However, dislocation densities were not measured in this work. Similarly, it can be noted that the denitrated mild steel (with an average grain size of 44 μm) is more sensitive to radiation exposure.

It is known that radiation-produced defects result in increased hardening which is expected to follow the square root dependence of the neutron fluence assuming that the concentration of radiation-produced defects is proportional to the fluence:

$$\Delta\sigma_{LY} = \sigma_{LY}^{irr} - \sigma_{LY}^0 = \alpha_1 Gb\sqrt{\rho} + \alpha_2 Gb\sqrt{2NR} = \alpha Gb\sqrt{\phi t}, \tag{3}$$

where the subscript LY stands for lower yield stress, superscript 'o' represents unirradiated sample, G is the shear modulus, b is the Burgers vector, ρ is the dislocation density (cm⁻²), N is the volume fraction of defects of radius R , α_1 and α_2 depend on the obstacle strength varying from 0 to 1, and α is a constant between 0.1 and 1. As shown earlier [12] the reduced sensitivity (one-third vs. one-half) to radiation can be rationalized through consideration of the two components, friction hardening and source hardening comprising the yield strength. While the friction stress follows the square root dependence, the source hardening decreases with neutron radiation due to the reduced interstitial atoms in solution.

3.2. Static strain aging

Fig. 4 includes typical unloading–loading tests on a single specimen to evaluate the strain aging index, f as defined in Eq. (1), while Fig. 5 shows the SSA index as a function of aging time for a vacuum annealed sample (grain size 27 μm) for several aging temperatures. The SSA index f indicates the extent of locking involved and is generally proportional to the number of interstitial atoms (N_t) removed from the original number (N_o) after time t . According to the Cottrell–Bilby model [13], $N_t \propto t^{2/3}$. Similarly, Bullough and Newman [14] and Ham [15] found a similar relationship at small t . On the other hand, Suzuki and Tomono [16] as well as McLennan and Hall [9] found that the aging time can be divided into two separate parts: for shorter times $N_t \propto t^{1.5}$, and at the longer times $N_t \propto t^{0.5}$. However, in the present study the data are too scattered for this type of relationship to be validated. All the experimental results are, however, better represented by a sigmoidal relationship given by

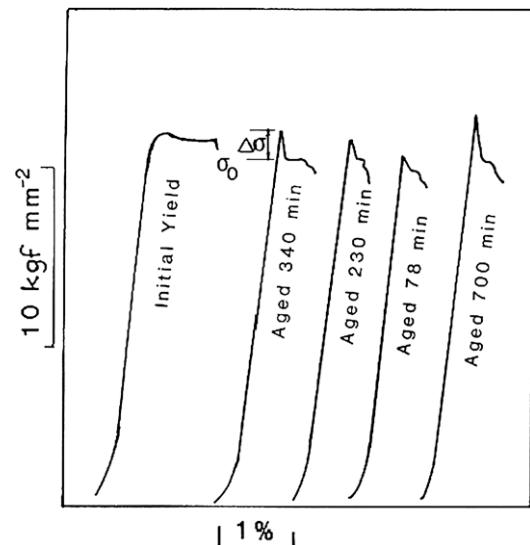


Fig. 4. An example of experimental method used in SSA studies (neutron dose 2.8 × 10¹⁷ n/cm², aging temperature 120 °C).

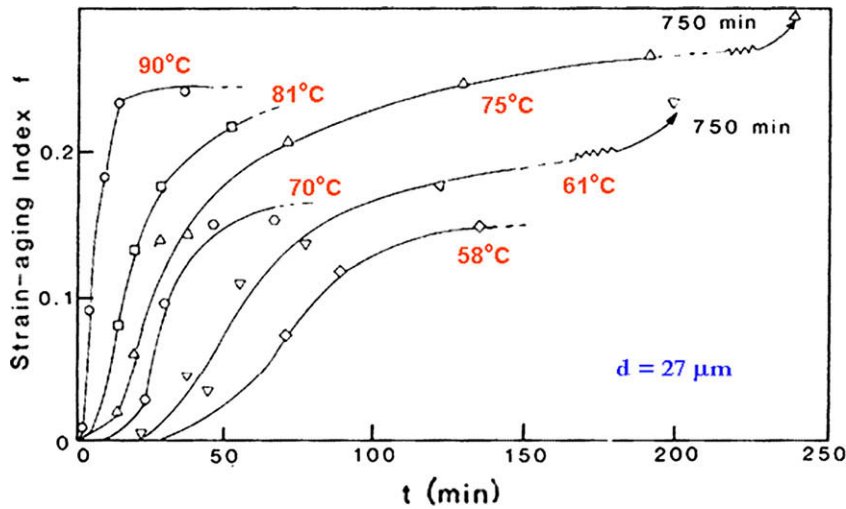


Fig. 5. SSA index vs. aging time for vacuum annealed samples at varied aging temperatures.

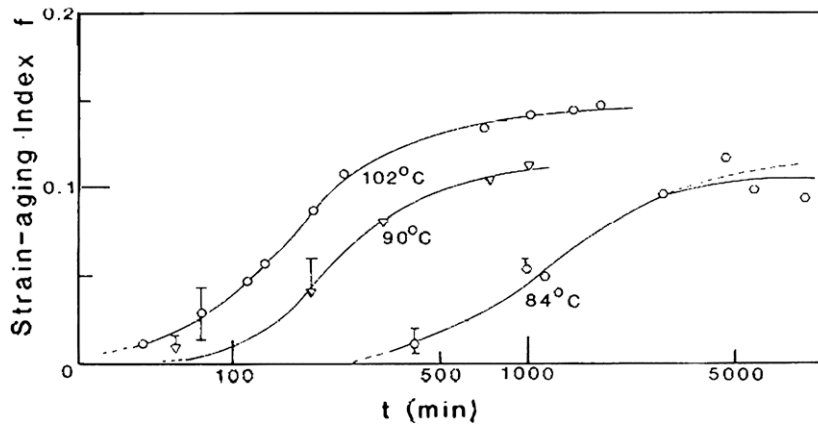


Fig. 6a. Effect of aging time on the SSA index for various aging temperatures in irradiated mild steel samples (neutron fluence, $2.8 \times 10^{17} \text{ n/cm}^2$).

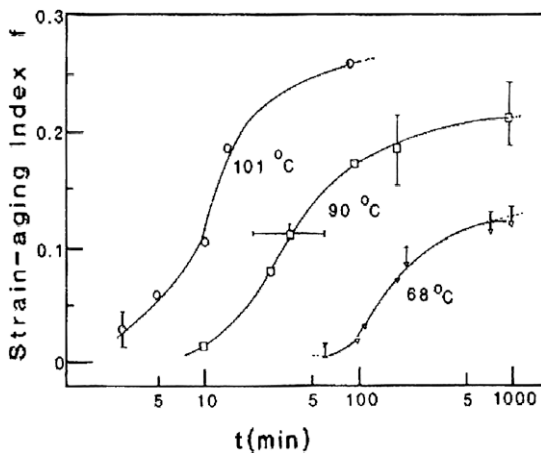


Fig. 6b. SSA index vs. aging time for a dry hydrogen treated (75 min at 675 °C) mild steel at various aging temperatures.

$2.8 \times 10^{17} \text{ n/cm}^2$. The data of f vs. aging time (min) are plotted for three different aging temperatures. It is shown that a higher temperature or aging time is needed to obtain the same f , i.e., the same degree of locking of interstitial atoms. Further, the data trend is similar to what was obtained for the vacuum annealed material (Fig. 5) with only one notable exception that rather longer aging times are required to obtain a similar f value. Quite similar effect was also noted for dry hydrogen treated mild steel specimens (Fig. 6(b)).

Fig. 7(a) shows the f index as a function of aging time for mild steel samples irradiated with three different fluences at a constant testing temperature of 90 °C. For irradiated steels, the extent of aging progressively decreases. It is important to note that the aging index becomes almost zero (i.e., the steel becomes essentially non-aging) irrespective of the aging time when the material was irradiated to a neutron fluence of $2.0 \times 10^{18} \text{ n/cm}^2$. Interestingly, similar behavior is observed in dry hydrogen treated specimens also. Fig. 7(b) shows aging index as a function of aging time for specimens treated for different times at a temperature of 90 °C. It is noted that a longer dry hydrogen treatment makes the steel progressively less aging, and when the steel is further treated in dry hydrogen for about 3 h, it became essentially non-aging.

The data generated from the SSA studies confirm that it is a thermally activated process. Fig. 8 shows an Arrhenius plot (aging time vs. inverse temperature) for various conditions (vacuum annealed,

$$f = 1 - \exp(-(t/\tau)^n), \quad (4)$$

where τ is a constant dependent on temperature [2].

The effect of neutron irradiation on the SSA index (f) is apparent from Fig. 6(a). The samples were irradiated to a neutron fluence of

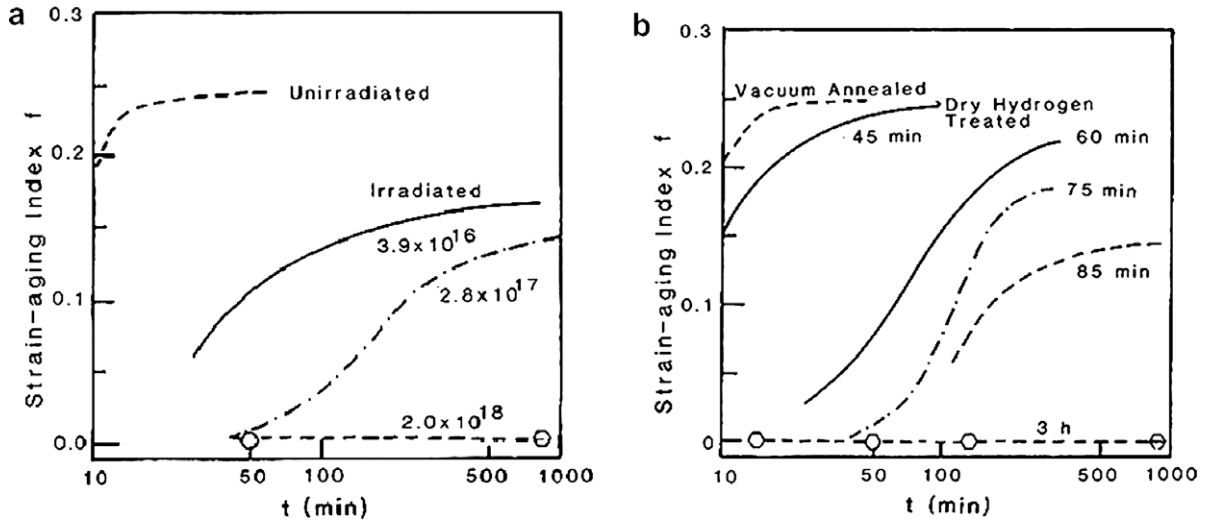


Fig. 7. The effect of (a) irradiation and (b) partial denitriding on SSA at 90 °C.

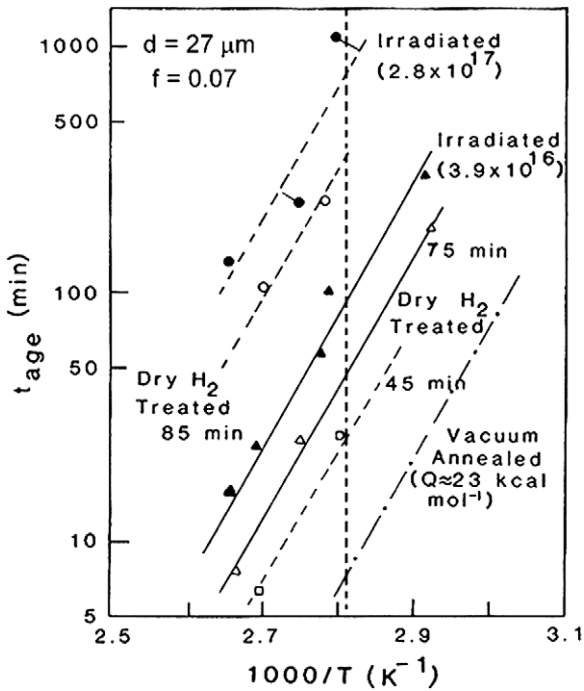


Fig. 8. Aging time vs. inverse temperature (Arrhenius plot) for different materials ($f = 0.07$).

irradiated and partially denitrided) of mild steel with a grain size of 27 μm for a particular value of SSA index (i.e., $f = 0.07$). Interestingly, the slope of these fitted lines is roughly the same. Thus, the activation energy of the process is evaluated to be 23.8 ± 3.2 kcal/mol which is in agreement with the values obtained in previous studies [6,7,9]. However, this value is greater than the activation energy of nitrogen or carbon atom diffusion in α -iron by about 5 kcal/mol. Similar results were obtained in the materials with other grain sizes. The discrepancy in the values has been attributed to the binding energy of nitrogen to manganese.

3.3. Effect of neutron fluence on nitrogen concentration

It has been postulated that upon neutron irradiation most interstitial impurities tend to form complexes with the radiation-pro-

duced defects, thus decreasing their net concentration in solution. But those impurity atoms in solution are important for locking up the mobile dislocations manifesting strain aging effects. It is generally considered to be exceedingly difficult to measure the interstitial impurity concentration in solution with confidence; McLennan and Hall [9] and Little and Harries [17] have used internal friction experiments that clearly indicated reduced concentration of interstitial impurities following radiation exposure.

It is clear from Table 1 that dry hydrogen treatment reduces the amount of nitrogen present in solution, and thus may simulate the effect of neutron irradiation on the nitrogen concentration. To analyze the situation for irradiated mild steel, we use the data in Fig. 8 to provide information about the equivalent aging time for an f value of 0.07 at an aging temperature of 80 °C (represented by the straight vertical line intersecting most of the parallel straight lines). In Fig. 8, the hydrogen treatment times are 45, 75 and 85 min while the nitrogen concentrations are known only for dry hydrogen treatments for 75 min and longer times (Table 1). However, the remaining 45 min (2.7 ks) and 85 min (5.1 ks) treatment data can be interpolated from the information given in Table 1 and Fig. 9. Now with the interpolated nitrogen concentration data and the data obtained for the hydrogen treated mild steel (from Fig. 8) we plot the nitrogen atom concentration vs. aging time in

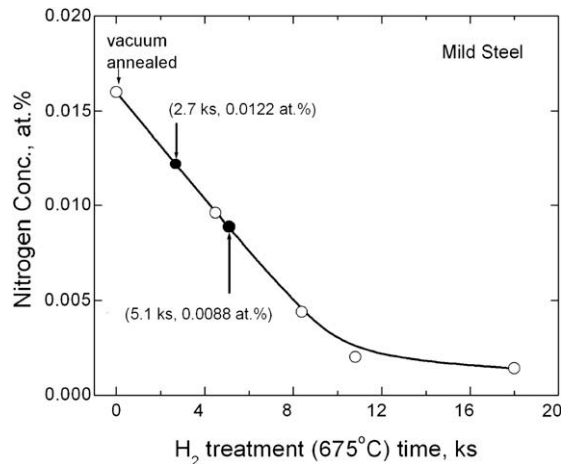


Fig. 9a. Nitrogen concentration against hydrogen treatment time at 675 °C.

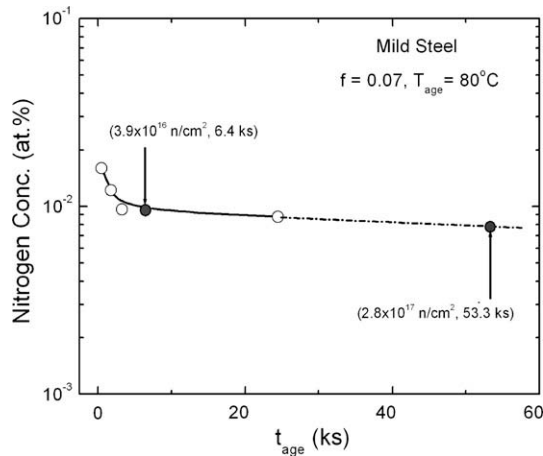


Fig. 9b. Nitrogen concentration as a function of aging time ($f=0.07$ and $T_{\text{age}}=80^{\circ}\text{C}$).

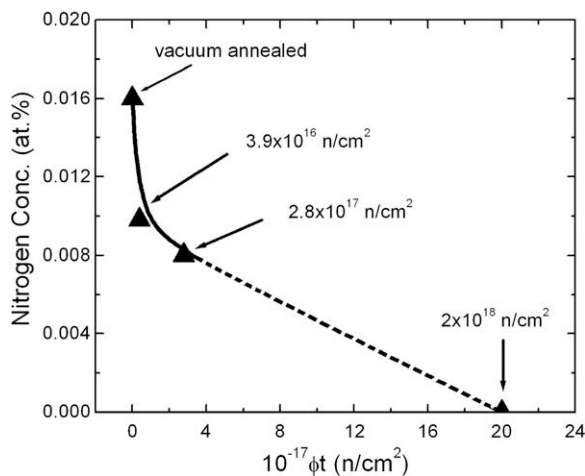


Fig. 10. The estimated nitrogen concentration as a function of neutron fluence in irradiated mild steel.

Fig. 9(b). The equivalent aging times for the irradiated steel from Fig. 8 are: 6.4 ks for a fluence of 3.9×10^{16} n/cm², and 53.3 ks for a fluence of 2.8×10^{17} n/cm². Their equivalent nitrogen concentrations are inter/extrapolated in Fig. 9(b). Therefore, now we have the data on the equivalent nitrogen atom concentration in solution for the irradiated mild steels as well.

Fig. 10 shows the results thus obtained along with the nitrogen concentration data of vacuum annealed sample; dashed line is an

extrapolation of the solid curve. It is interesting to observe that the curve follows a trend in such a way that at a fluence of $\sim 2 \times 10^{18}$ n/cm², the equivalent nitrogen concentration becomes nil. As stated previously, the mild steel becomes essentially non-aging under similar neutron fluence. Although the nitrogen concentration data used are rather average total concentrations, not exactly the concentration in solution, it does give a reasonable estimation of the trend and is consistent with the hypothesis that the effective nitrogen concentration in irradiated mild steel goes down. It will be useful to obtain data using other techniques such as internal friction, thermoelectric power (Seebeck coefficient), electrical resistivity, etc. on irradiated steel for a quantitative correlation to the current extrapolated results.

4. Conclusions

The effects of neutron irradiation and dry hydrogen treatment on the yield point phenomena in mild steel were investigated. SSA studies revealed a complex time dependence of the SSA index (f). The effect of neutron irradiation was found to decrease the effect of aging and at high fluences, a non-aging steel was obtained. Importantly, the mechanism of strain aging is not affected by neutron irradiation (and dry hydrogen treatment). With the data available, it is convincingly shown that the neutron irradiation actually causes the nitrogen concentration to decrease in solution, making them less susceptible to the strain aging effects.

Acknowledgments

We gratefully acknowledge the support of the DOE Grant DE-FG07-041D14611. We express our appreciation to the reviewers for many useful comments.

References

- [1] G.E. Dieter, Mechanical Metallurgy, McGraw-Hill Book Company, New York, 1961.
- [2] E.O. Hall, Yield Point Phenomenon in Metals and Alloys, Macmillan, London, 1970.
- [3] J.D. Baird, Metallurgical Reviews, Review No. 149.
- [4] K.L. Murty, E.O. Hall, in: Irradiation Effects on the Microstructure and Properties of Metals, vol. 611, ASTM STP, 1976, p. 53.
- [5] I. Charit, C.S. Seok, K.L. Murty, J. Nucl. Mater. 361 (2007) 262.
- [6] W. Sylwestrowicz, E.O. Hall, Proc. Phys. Soc., London, Sec. B 64 (1951) 495.
- [7] J.S. Blakemore, E.O. Hall, J. Aust. Inst. Met. 8 (1963) 191.
- [8] M.S. Wechsler, J. Eng. Mater. Technol. 101 (1979) 114.
- [9] J.E. McLennan, E.O. Hall, J. Aust. Inst. Met. 8 (1963) 191.
- [10] K.L. Murty, Mater. Sci. Eng. 59 (1983) 207.
- [11] M.A. Adams, J. Sci. Instrum. 36 (1959) 444.
- [12] K.L. Murty, D.J. Oh, Scripta Metall. 17 (1983) 317.
- [13] A.H. Cottrell, B.A. Bilby, Proc. R Soc. London, Sec. A 62 (1949) 49.
- [14] R. Bullough, R.C. Newman, Proc. R Soc. London, Ser. A 266 (1962) 189.
- [15] F.S. Ham, J. Appl. Phys. 30 (1959) 915.
- [16] T. Suzuki, Y. Tomono, J. Phys. Soc. Jpn. 14 (1959) 597.
- [17] E.A. Little, D.R. Harries, Met. Sci. J. 4 (1970) 195.